Magazine of Civil Engineering

ISSN 2712-8172

journal homepage: http://engstroy.spbstu.ru/

Research article

UDC 691.3

DOI: 10.34910/MCE.140.3

Durability of ultra-high-performance concrete with silica fume and rice husk ash

E.O. Ferreira , ***A.T. Maia*** , ***W. Mazer*** ✉

Federal Technological University of Parana, Parana, Brazil

✉ *wmazer@utfpr.edu.br*

Keywords: ultra-high performance concrete, durability, silica fume, rice husk ash, high temperature.

Abstract. This study analyzed the behavior of Ultra-high performance concrete (UHPC) with two different pozzolans: silica fume and rice husk ash. The use of UHPC as a structural repair material has become common, making it necessary to evaluate its behavior in these situations. The study was conducted by determining compressive strength, assessing permeability and porosity, and assessing its behavior against sulfate attack and exposure to high temperatures. The compressive strength of the concretes was greater than 130 MPa. Regarding porosity and permeability, the concrete composed of silica fume exhibits approximately 20 % lower water absorption than those molded with rice husk ash. Analyzing sulfate attack, the concrete composed of rice husk ash exhibited approximately 50 % lower sulfate penetration than the silica fume composites. The performance of the materials, when subjected to temperatures of 200 and 300 °C, showed reductions in mechanical strength of approximately 26 and 36 %, respectively. At a temperature of 400 °C, the spalling phenomenon occurred. Therefore, there is potential for the use of such a composite due to its high mechanical strength and good performance in relevant characteristics, related to low permeability and high durability.

Acknowledgments. The authors would like to thank CAPES – Coordination for the Improvement of Higher Education Personnel and the Graduate Program in Engineering from the Federal Technology University of Paraná who collectively financed this project.

We thank the Multi-User Center for Materials Characterization – CMCM of UTFPR-CT for carrying out the SEM and DES tests.

Citation: Ferreira, E.O.F., Maia, A.T.M., Mazer, W.M. Durability of ultra-high-performance concrete with silica fume and rice husk ash. Magazine of Civil Engineering. 2025. 18(8). Article no. 14003. DOI: 10.34910/MCE.140.3

1. Introduction

Ultra high-performance concrete (UHPC) is a concrete that has high cement content, aggregates of reduced dimensions, high mechanical strength, and low permeability, has been gaining prominence, with the increased use of mineral admixtures such as silica fume (SF) and rice husk ash (RHA). SF is a product from the production process of the ferrosilicon and iron metallic industries and RHA is considered a residue from the controlled burning of rice husks during the processing of this cereal. Both additions, due to the high silica content in their composition, become materials with high pozzolanic activity, improving the microstructure and mechanical resistance of UHPC [1].

Several studies have been carried out to disseminate the use of UHPC as a structural recovery material in reinforced concrete buildings that present damage that could compromise the safety of the building and users, increasing its durability and restoring its useful life [2–4].

With the interest in spreading the use of UHPC as a material for the rehabilitation of structures, understanding its behavior in terms of durability becomes relevant because it presents itself as a material of very low permeability, preventing the entry of aggressive agents and improving mechanical resistance [2].

The alternative application of UHPC as a recovery material has been studied because it presents better performance against aggressive environmental actions, as shown by the works of Chen et al. [5], Bajaber and Hakeem [6], and Li et al. [7] and high velocity impact [8]. Also, according to Tayeh et al. [2], UHPC require less working time to carry out their application when they exhibit self-compacting behavior, increase the durability and life expectancy of repaired structures, and require fewer preventive actions.

Its mechanical characteristics for UHPC, and its resistance values obtained within the interval of 28 and 90 days are likely to measure the growth gain for this material [9]. Due to its low permeability, UHPC in situations prone to attack by sulfates has a lower deterioration rate than conventional concretes [6, 10–12].

Due to its dense microstructure, when UHPC is subjected to high temperatures, it exhibits explosive behavior. However, this type of sudden shattering phenomenon is controlled with the use of mineral additions and fiber incorporation in cementitious composites [13, 14].

Given the various variations in the availability of pozzolanic materials, this work aims to contribute to the study of UHPCs composed of pozzolans available in Brazil to encourage research and application of this type of product.

2. Materials and Methods

2.1. Materials

The concretes were made with Portland cement CP V – ARI. The cement was characterized and had a specific mass of 3.07 g/cm^3 and a specific surface area of 379.0 m^2/kg.

The RHA used has a specific mass of 2.16 g/cm^3 and a specific surface area of 345.8 m^2/kg obtained by the BETTERSIZE/S3 PLUS laser particle analyzer with an analysis range of 0.01 to 3500 μm by wet method using distilled water.

The quartz powder (QP) used in this research, according to the manufacturer, has a specific mass of 2500 kg/m^3.

For the granulometry of SF, the results of D(10), D(50), and D(90) are 4.92, 14.0, and 32.72 μm, respectively. With this, it was identified that the average diameter of the material is greater than that addressed in the literature – in the order of 0.2 μm – this occurs for other authors such as Romano et al. [15] and Fraga et al. [16], where, according to them, in situations where the SF presents particle agglomeration, the diameters are not congruent with those specified by the manufacturer, as the grains of the material agglomerate resulting in a grain of greater diameter, and do not undergo full use and reactive potential in the mixtures, affecting the formation of C-S-H gel through the consumption of free calcium hydroxide in the mixtures.

The particle size composition of this research is shown in Fig. 1.

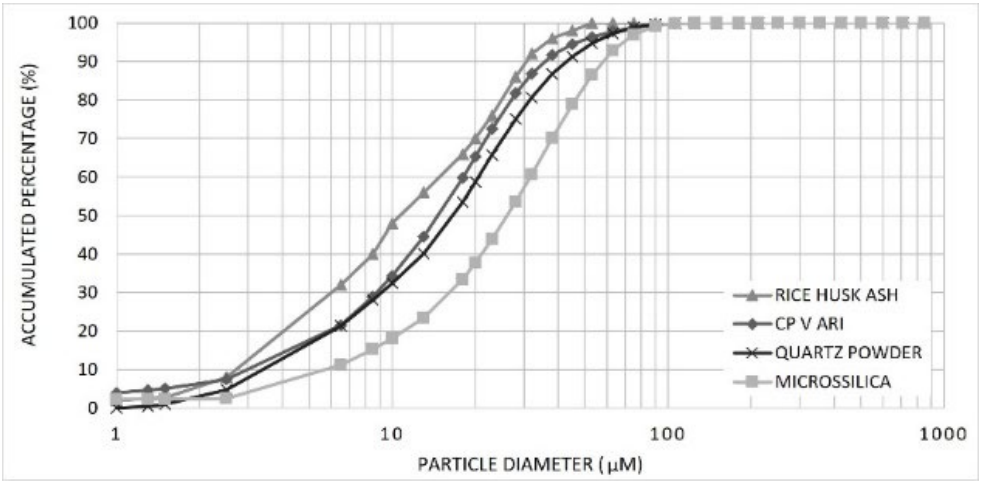

Figure 1. Granulometry of powdery materials.

According to X-ray diffractometry, cementitious and pozzolanic materials demonstrate different structures, as shown in Fig. 2 and Table 1. The test detected that for QP, there is a crystalline structure since it is possible to identify an intense peak. As for the materials CP-V ARI cement, SF and RHA, these have graphs with low intensities, this representation indicates that the products have an amorphous structure.

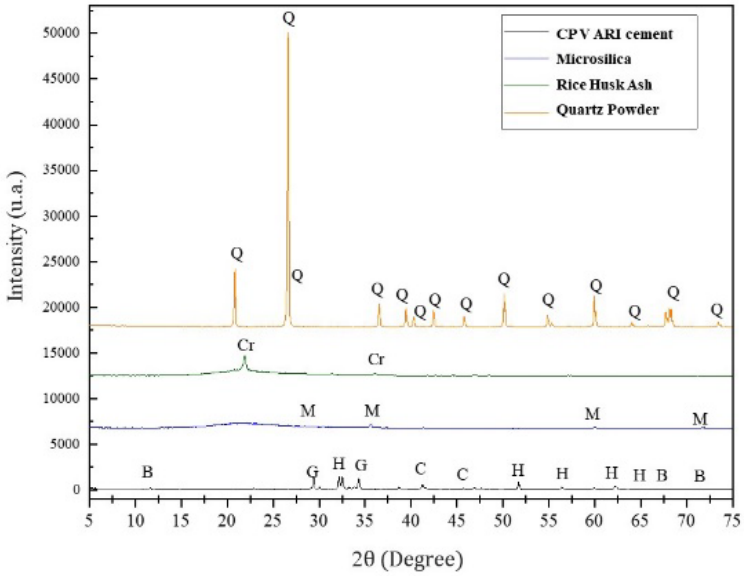

Figure 2. X-ray diffraction (XRD) results for CP V ARI cement, SF, RHA, and QP.

Table 1. XRD results for cement, QP, SF, and RHA.

Mineral	Chemical formula	Acronym	Cement	QP	SF	RHA
Quartz	SiO_2	Q/M	–	100	100	–
Cristobalite	SiO_2	Cr	–	–	–	100
Calcite	$CaCO_3$	C	20	–	–	–
C_3S	Ca_3SiO_5	H	67	–	–	–
Brownmillerita	Ca_2FeAlO_5	B	7	–	–	–
Gypsum	$CaSO_4.2H_2O$	G	6	–	–	–

The packaging of two grains of sand with different granulometries was prepared, where they were dosed according to the packaging based on the Equation Andreasen and Andersen modified adopting q = = 0.37, and the granulometric curve obtained shown in Fig. 3.

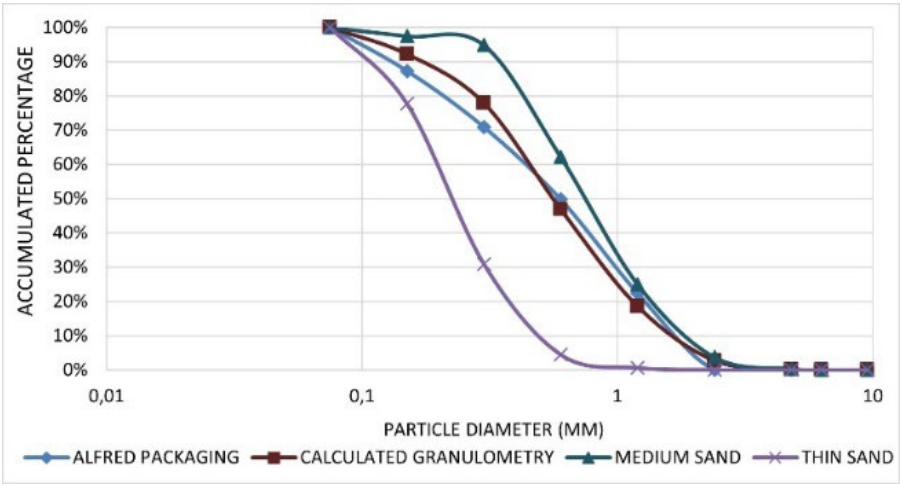

Figure 3. Particle packing according to the modified Andreasen and Andersen model.

A superplasticizer based on polycarboxylate ether with a specific mass of 1.120 g/cm^3 was used 4 % of the mass of the cement. The mix design is showed in Table 2.

Table 2. Concrete mix design.

Material	Cement	Fine sand	Medium sand	QP	SF	RHA	Water	Superplasticizer
Mix 1 (kg/m^3)	855	204	578	239	195	–	197	42
Mix 2 (kg/m^3)	861	204	578	230	–	189	197	42

2.2. Methods

2.2.1. Compression tests

The UHPCs were tested according to NBR 5739 – Concrete – Compression tests of cylindrical specimens [17] to determine the resistance to compression, using six samples submitted to the axial compression test in a press with a capacity of 200 kN with a test speed of 0.45 MPa/s, performing tests at ages of 28 and 90 days.

2.2.2. Water absorption capacity

To analyze the water absorption capacity and determine the void ratio, the methodology described by NBR 9778 – Hardened mortar and concrete – Determination of water absorption, void ratio, and specific mass [18] was adopted. in which, for each mixture with different pozzolanic materials, six samples were manufactured and submitted to the test at the age of 90 days.

The test started with the drying of the specimens in an oven at 105 °C for 24 hours. Subsequently, successive weighings were carried out until the difference in mass between two weighings was less than 1 %. After that, the dry mass (ms) of each sample was determined and then submerged in water for 72 hours. After this time, the specimens were submerged in another container where the temperature was raised to boiling point for 5 hours and after cooling down completely, the submerged mass was determined using the hydrostatic balance (mi). At the end of the test, the saturated mass was also measured in the dry surface condition $(msat)$.

At the end, the water absorption (A) was determined using Equation 1:

$$A = \frac{msat - ms}{ms} * 100. \tag{1}$$

We obtained the void ratio (VR) according to Equation 2:

$$VR = \frac{msat - ms}{msat - mi} * 100. \tag{2}$$

The specific mass was determined by Equation 3:

$$pr = \frac{ms}{ms - mi} * 100. \tag{3}$$

2.2.3. Absorption of water by capillarity

Initially, the samples were dried in an oven at 105 °C until constant mass, and the dry mass of the samples (ms) was determined. Then, the sides of the specimens were sealed with epoxy paint, and the samples were placed on a rack in a container of water until the water level covered a height of 5 mm from the samples. According to the procedures of NBR 9779 [19], the samples were weighed after 3, 6, 24, 48, and 72 h, at which point the saturated mass $(msast)$ was determined. After the last weighing, the specimens were broken diametrically to measure the capillary rise in each sample.

The final result of water absorption is calculated according to Equation 4, where S means the cross-sectional area of the sample in contact with water, and a visual analysis of the water percolation profile inside the concrete is carried out as required by NBR 9779 [19]:

$$C = \frac{msast - ms}{S}. \tag{4}$$

2.2.4. Attacks of sulfates – magnesium

The methodology for determining the attack of sulfates in concrete is based on measuring the expansion of prismatic specimens subjected to an environment saturated with sulfates over a period at high temperatures, however, this technique requires approximately two years to obtain results [20].

The concrete portions of each specimen were dried in an oven for 8 hours at 100 °C and after removing from the oven and reaching room temperature, each sample was ground in a pan mill until the particles reached a diameter less than 150 μm, which are used to determine the amount of sulfates in each sample.

The sulfate content of the samples is determined according to Equation 5, described by NBR16937-6 – Aggressive waters – Durability of concrete – Part 6: Determination of sulfate soluble in water [21]:

$$SO_4^{-2} = \frac{\text{Mcalcined} \times 0.4116}{\text{Mcollected}} \times 100, \quad (5)$$

where 0.4116 = is the conversion factor of barium sulfate to sulfate ion $\left(SO_4^{-2}\right)$.

2.2.5. Influence of temperature increase on axial compressive strength

NBR 14432 – Fire resistance requirements for building construction elements – Procedure [22] describes the required fire resistance time of a maximum of 120 minutes, therefore, for this test, 18 specimens were prepared, of which divided into three groups for three different temperatures. The test specimens underwent submerged curing and at the age of 28 days they were removed from the water and kept in a chamber for 10 days so that the moisture content was reduced until reaching hygroscopic equilibrium with the environment [23].

To carry out the tests at temperatures of 200, 300, and 400 °C, the concretes of each analysis group were subjected to heating at a rate of 10 °C/min in a muffle furnace until the temperature established for each set analyzed, which were then maintained for 120 continuous minutes under the action of high temperature, and, after heating, the samples were naturally cooled inside the muffle until they reached room temperature.

Representing the standard fire curve, Fig. 4 shows that during the heating period, there is a continuous rise and temperature uniformity (T) within 120 minutes, between t_1 and t_2, as determined by NBR 14432 [22].

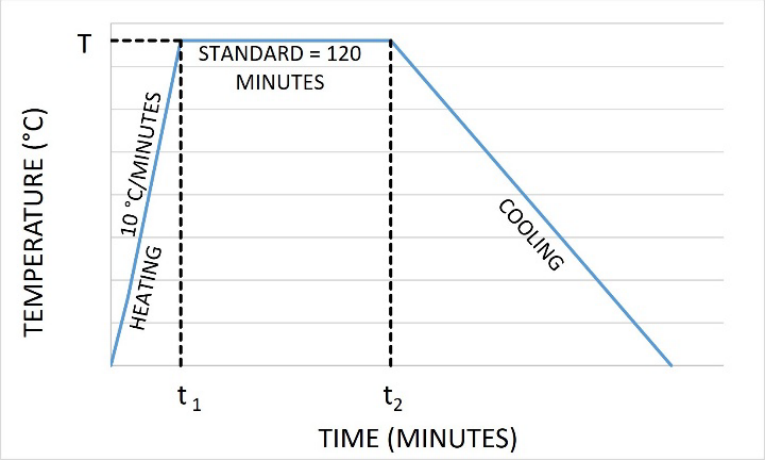

Figure 4. Heating scheme for the temperature influence test.

To characterize the effect of high temperatures on UHPC, axial compression tests were carried out to identify the influence on the mechanical properties of the material [24–26].

2.2.6. X-Ray diffraction test

X-ray diffraction is a test where it is possible to characterize the crystalline structure of materials using Shimadzu's XRD 7000 equipment. The equipment software detects the intensity at the peak position, the interplanar distance, and the peak width.

3. Results and Dicussion

3.1. Compression Tests

The axial compression results were obtained according to the methodology determined by NBR 5739 [17] and the method of statistical refinement of Peirce's treatment was used to determine the final values of resistance to compression, presented in Fig. 5.

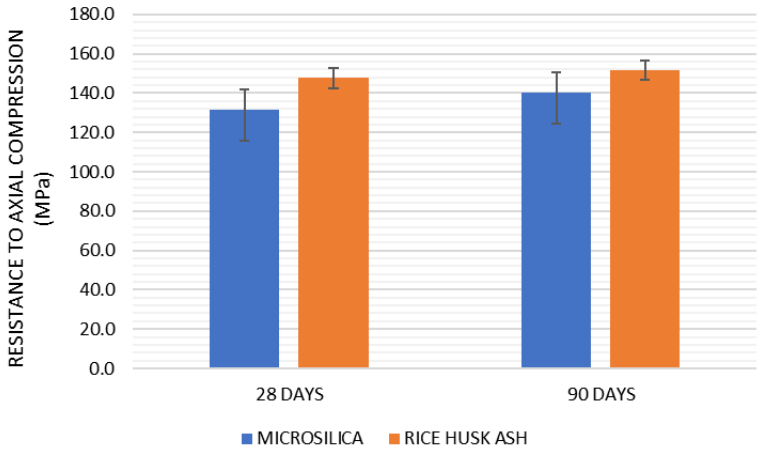

Figure 5. Comparison between strengths at different test ages.

With the results obtained, it is possible to identify that for concretes composed of RHA, the resistance to axial compression was about 8 % higher than in comparison to concretes with SF. Given the results, between the ages of 28 to 90 days, the strength gain for SF concretes was 8 % and approximately 3 % for concretes with RHA. The results shown in Fig. 5 show that after 90 days, there was a strength gain of around 7 and 3 % for concrete cast with SF and with RHA, respectively, as also shown in Table 3.

Table 3. Axial compression results for UHPC.

Specimen	SF	RHA	SF	RHA
Age	**28 days**		**90 days**	
Average (MPa)	131.39	147.62	140.41	151.73
Standard deviation (MPa)	10.39	5.05	15.85	3.66
Coefficient of variation (%)	7.91	3.42	11.29	2.41

Based on the methodology for the statistical analysis of UHPC using the analysis of variance for different sample sizes, at the 95 % confidence interval, it is possible to observe the compressive strength of the concretes composed of SF at 28 days is equal to the results obtained at 90 days and equal to the compressive strength of the samples with RHA at 28 days.

The compressive strength with SF at 28 days is equal to 90 days and is also equal to the compressive strength with RHA at 28 days. In both concrete, even with the variation of its pozzolanic addition, it was not possible to observe a significant difference in the compressive strength gain between the ages of 28 and 90 days, in addition to that, there was no difference between the strengths with different mineral additions for a same age. The values obtained are higher than the values observed by Bulgakov et al. [27] and by Lesovik et al. [28], who used SF.

3.2. Water Absorption Capacity and Void Index

For the test described by NBR 9778 [18], each group composed of six specimens was submitted to the water absorption test at the age of 90 days. The results of absorption by immersion and the voids index are shown in Table 4.

Table 4. Results of the absorption test by immersion of the voids index.

Specimen	SF		RHA	
Test	**Absorption**	**Voids index**	**Absorption**	**Voids index**
Average (%)	2.02	4.53	1.98	4.39
Standard deviation (%)	0.13	0.33	0.19	0.41
Coefficient of variation (%)	6.39	7.39	9.58	9.28

Through statistical analysis, for concretes molded with SF, the average water absorption was 2.02 %, and for concretes with RHA, it was 1.98 %, as shown in Table 3, indicating that both results equal a 95 % confidence index. As for the voids index, with the average result obtained for SF of 4.53 % and for concretes consisting of RHA of 4.39 %, both are statistically equal to a confidence index of 95 % according to the analysis of variance.

According to Dinakar et al. [29] and Medeiros-Junior et al. [30], concretes with levels of water absorption by immersion after 72 hours below 3 % are considered good in the aspect of low infiltration capacity, thus being able to state that for concretes molded we have a low absorption rate, with values slightly lower than those observed by [27].

3.3. Absorption of Water by Capillarity

The test described by NBR 9779 [18] was performed on six concrete samples for each pozzolan analyzed to determine the average values of capillary absorption at the age of 90 days. The results are shown in Table 5.

Table 5. Results of the capillary absorption test.

Specimen	SF	RHA
Average (%)	0.065	0.082
Standard deviation (%)	0.005	0.003

Graphically, Fig. 6 shows the correlation between absorption over test times.

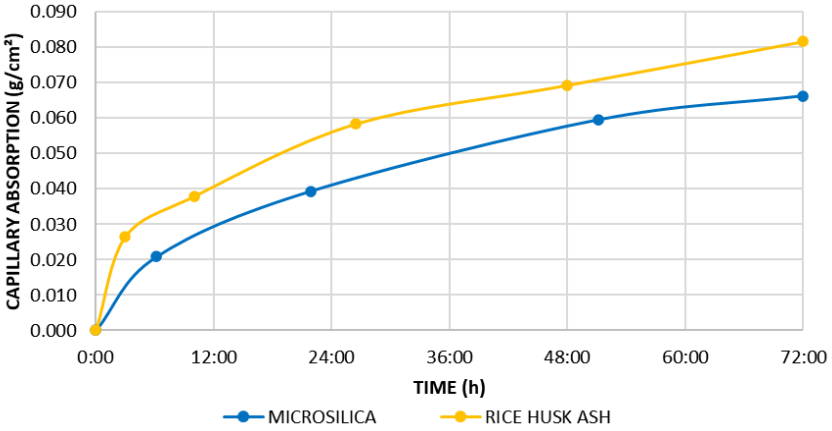

Figure 6. Absorption by capillarity as determined by NBR 9779 [18].

It is possible to identify in Fig. 6 that the water content absorbed by capillarity increased as the test time elapsed in both mixtures. Note that there is a tendency for absorption to stabilize due to the maximum absorption rate of the material.

It is possible to identify that concretes made with RHA tend to have an absorption rate of approximately 20 % more than those molded with SF, demonstrating that this pozzolan has a more porous matrix that allows greater water flow through the composite, such effect is corroborated with the analysis of variance at a confidence index of 95 %, which demonstrates a statistical difference in the permeability content for concretes with different pozzolanic additions.

This analysis had already been described previously since the criterion that the pores are connected and have different dimensions for each type of material, influencing the effective capacity to resist the penetration of water in the cementitious matrix.

3.4. Attacks of Sulfates – Magnesium

To measure the attack content of sulfates in UHPC made with SF, after the test, the results are presented in Table 6.

Table 6. Results obtained for the sulfate content test.

Specimen	SF	RHA
Average (%)	1.417	0.942
Standard deviation (%)	0.297	0.088

Table 6 presents the result of the average value of sulfate attack content for concretes with SF being 1.417 % and for concretes with RHA of 0.942 %. Due to the lack of parameters for this material, Mazer et al. [20] indicate that for concrete, contents above the 0.46 % limit already indicate the existence of significant penetration of sulfates in the structure, whereas Sun et al. [31], in solutions with 50 g/l, the sulfate content was 0.329 % due to the normalization of the concentration due to the rapid formation of gypsum and ettringite in the pores, which prevented a greater penetration of ions inside the concrete. With this, it is possible to state that in concrete composed of SF, there is a propensity of approximately 50 % of this type of material to suffer from the penetration of sulfates in its structure.

To correlate the results of the penetration of sulfates with the permeability of the materials, Fig. 7 demonstrates that for concrete made with SF, the tendency for penetration of sulfate ions is lower than for composite concrete by RHA.

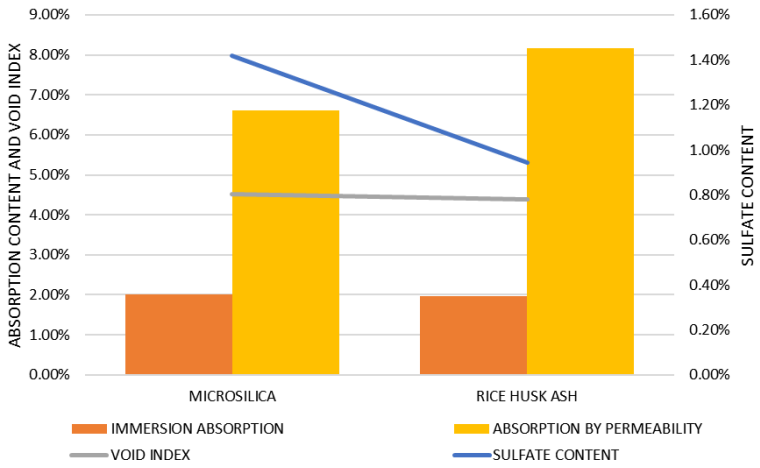

Figure 7. Correlation between sulfate absorption and penetration levels.

According to Sun et. al. [31] and Zou et al. [32] at a higher solution concentration, more sulfate ions penetrate the concrete for the same immersion time, with this, the correlation between the absorption rate of the material and the lowest. The value of penetration of sulfate ions into concrete is because in the initial stage of the attack, the expansive products fill the pores of the materials and prevent the transport of sulfate ions.

Regarding the mechanical resistance of the specimens submitted to the sulfate attack test, Table 7 presents the results obtained in the axial compression test of the specimens after 90 days of testing.

Table 7. Compression results of UHPC after sulfate attack.

Specimen	SF	RHA
Average (MPa)	85.55	85.34
Standard deviation (MPa)	12.19	15.32
Coefficient of variation (%)	14.25	17.96

According to the results of Table 7, it is possible to identify the influence of sulfate attack on the concrete structure in terms of mechanical strength since, compared to the results obtained in Table 1, there was a decrease in the resistance to axial compression of 60 % for the UHPC molded with SF and of 56 % for the specimens constituted of RHA.

Such results corroborate the difference in the sulfate content penetrated in the samples since the ratio between the sulfate penetration content and the axial compression strength for concretes with SF is 0.016 and for concretes with RHA is 0.011, indicating a greater propensity to occur with the first pozzolan analyzed, statistically confirmed by the analysis of variance with 95 % confidence where for concretes with RHA they have less penetration of sulfates.

Using the analysis of variance criterion to determine the resistance to sulfate attack, the compressive strengths of concrete submitted to the sulfate attack test, regardless of the type of addition used, present statistically equal values with 95 % confidence, that there is a reduction in resistance about the reference concretes of the same age since they are statistically different. This factor can be explained by the reactions that occur in the cementitious matrix of UHPC molded with RHA, in which the sulfates reacted in the most superficial pores, preventing the progression of the action into the material.

3.5. Influence of Temperature Increase on Axial Compressive Strength

The first group of samples was subjected to heating at a temperature of 200 °C and after cooling, they were subjected to the axial compression test to determine the mechanical resistance of the UHPC, as shown in Table 8.

Table 8. Compression results of the heating test up to 200 °C.

Specimen	SF	RHA
Average (MPa)	89.83	109.44
Standard deviation (MPa)	29.72	8.13
Coefficient of variation (%)	33.10	7.43

For the samples subjected to 300 °C, the specimens with SF did not show visible signs of degradation or chipping, however, two samples of the concrete molded with RHA suffered from the spalling phenomenon. Its compressive strength results are shown in Table 9.

Table 9. Compression results of the heating test up to 300°C.

Specimen	SF	RHA
Average (MPa)	79.95	105.17
Standard deviation (MPa)	14.21	13.37
Coefficient of variation (%)	17.77	8.99

The samples subjected to heating up to 400 °C had the spalling phenomenon evident and already described by Abid et al. [13], it was not possible to perform the mechanical resistance test on the specimens.

According to Tables 8 and 9, the compressive strength of UHPC composed of SF elevated at 200 and 300 °C are statistically different from the reference compressive strength, indicating a loss of strength of 31.6 and 39.2 %, respectively, but the resistances at 200 and 300 °C are equal.

The compressive strength, heated to 200 and 300 °C, with RHA, are statistically different from the reference compressive strength, indicating a loss of strength of 25.9 and 28.7 %, respectively, but the strengths at 200 and 300 °C are equal.

Changing the type of addition shows a difference in the compressive strength between them for the same temperature, that is, concretes with SF show a greater loss of strength than in comparison with UHPC that use RHA. Two RHA samples exhibited spalling at a temperature of 300 °C, likely because they have a higher capillary absorption coefficient than the SF samples, indicating finer pores, which resulted in a greater capillary height. Additionally, the RHA samples also have a lower void ratio, hindering water escape from their interior. The combination of these effects may have caused spalling in both samples. However, the remaining intact samples showed less strength loss compared to the reference samples, when compared to the strength loss of the SF samples.

3.6. X-Ray Diffraction Test

The results of changes in the microstructures of concretes made of SF pozzolan are shown in Fig. 8.

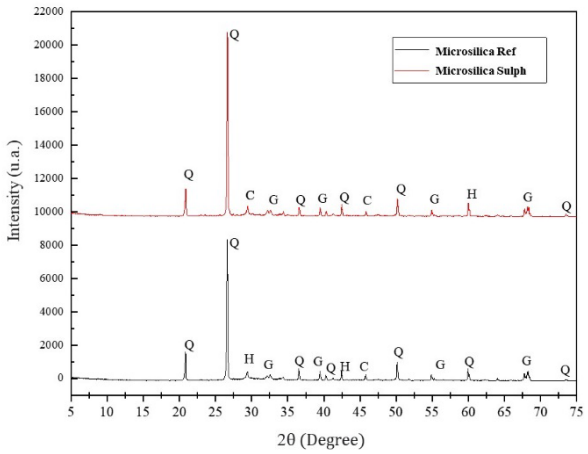

Figure 8. XRD results for reference concrete with SF compared to concrete subjected to sulfate attack.

As seen in Fig. 8, the peaks for the UHPC with reference SF (SF Ref) in comparison with the SF concrete subjected to sulfate attack (SF Sulph) are similar, and their mineralogical percentages are shown in Table 10.

Table 10. XRD result for reference concretes with SF compared to concretes subjected to sulfate attack.

Mineral	Chemical formula	Acronym	SF Ref	SF Sulph
Quartz	SiO_2	Q	56	53
Tobermorite	$Ca_5Si_6O_{16}(OH)_2.4H_2O$	T	30	38
Portlandite	$Ca(OH)_2$	P	0	0
Ettringite	$3CaO.Al_2O_3.3CaSO_4.32H_2O$	E	11	1
Gypsum	$CaSO_4.2H_2O$	G	3	8

According to Table 10, the presence of sulfate ions resulted in an increase in the gypsum content of concrete subjected to this type of exposure, as described by Zou et al. [32]. Despite the samples being subjected to Mg sulfate attack, the exposure time, the low void content and the low water/binder ratio did not allow the material to decompose to a chemically identifiable degree.

Fig. 9 together with Table 11 shows the results of the XRD test for the concretes using SF Ref and when molded with the same pozzolan but submitted to 200, 300, and 400 °C, being represented by SF 200°C, SF 300 °C, and SF 400 °C, respectively.

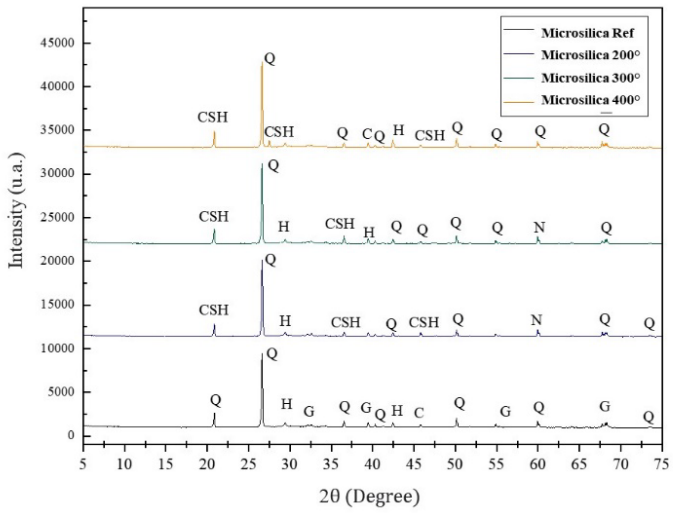

Figure 9. XRD results for reference concrete with SF compared to concretes subjected to different temperature rises.

Table 11. XRD results for reference concretes with SF compared to concretes subjected to different temperature rises.

Mineral	Chemical formula	Acronym	SF Ref	SF 200°	SF 300°	SF 400°
Quartz	SiO_2	Q	56	57	64	61
Tobermorite	$Ca_5Si_6O_{16}(OH)_2.4H_2O$	T	30	23	16	14
Portlandite	$Ca(OH)_2$	P	0	0	1	1
Ettringite	$3CaO.Al_2O_3.3CaSO_4.32H_2O$	E	11	18	16	23
Gypsum	$CaSO_4.2H_2O$	G	3	2	2	1

Concretes subjected to different temperature gradients show some changes in the final chemical composition about the reference, and for samples subjected to temperatures above 200 °C, it is possible to identify that there is a reduction in the Van Der Walls forces and the C-S-H of material. From 200 °C, the water chemically linked to the C-S-H (tobermorite) is lost, which can be identified by the increase in the free SiO_2 content in the structure, the decrease in the tobermorite content and the decomposition of the gypsum. With this, the mechanical strength of the material was compromised as shown in the results of resistance to axial compression previously.

For concrete made of RHA, the results of the XRD test are presented in Fig. 10 and the mineralogical percentages are described in Table 12, where it is possible to identify that the peaks of greater intensities coincide both between the reference concrete (RHA Ref) for this pozzolan as well as for concrete subjected to sulfate attack (RHA Sulph).

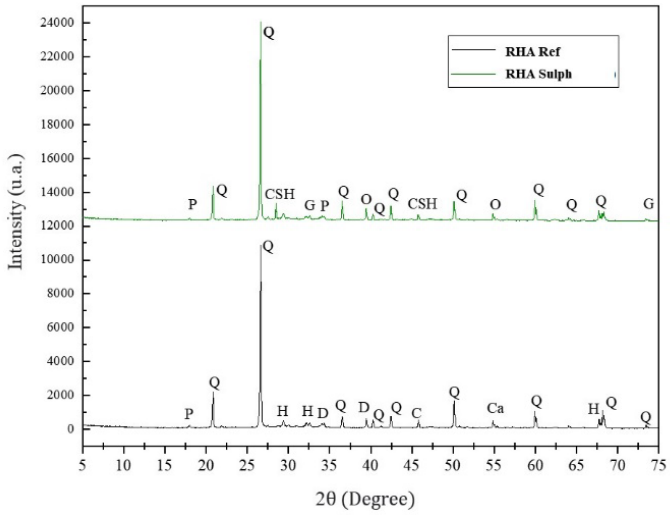

Figure 10. XRD results for the reference concretes with RHA compared to the concrete subjected to sulfate attack.

Table 12. XRD test results for concretes with RHA after sulfate test.

Mineral	Chemical formula	Acronym	RHA Ref	RHA Sulph
Quartz	SiO_2	Q	46	50
Tobermorite	$Ca_5Si_6O_{16}(OH)_2.4H_2O$	T	32	31
Portlandite	$Ca(OH)_2$	P	1	1
Ettringite	$3CaO.Al_2O_3.3CaSO_4.32H_2O$	E	15	13
Gypsum	$CaSO_4.2H_2O$	G	6	5

Table 12 presents the minerals formed based on Fig. 10, where the highest mineral percentage is silica in both analyzed samples. For the RHA Sulph and RHA Ref samples, the low rate of change in the ettringite content may be a consequence of hydration reactions due to the heat treatment to which the samples were subjected, preventing chemical changes in the UHPC compounds.

Concrete molded with RHA pozzolan (RHA Ref) together with concrete of the same pozzolan subjected to 200, 300, and 400 °C have the values shown in Fig. 11 as XRD test results and in Table 13, with the samples RHA 200 °C, RHA 300 °C, and RHA 400 °C abbreviations referring to each temperature to which the samples were submitted.

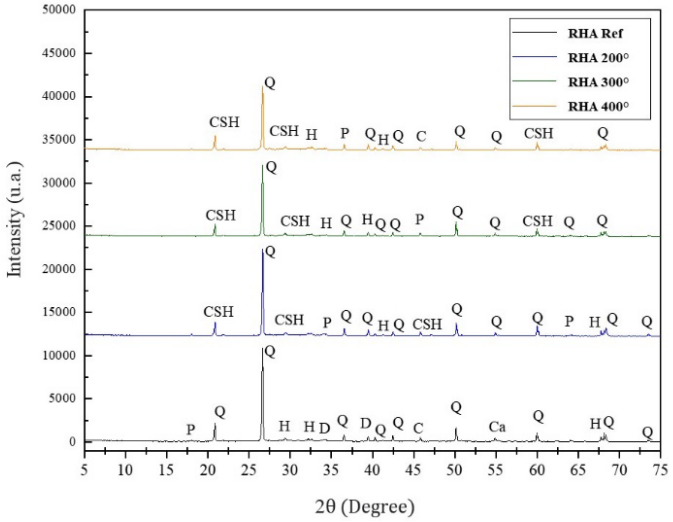

Figure 11. XRD results for reference concretes with RHA compared to concretes submitted to different temperature rises.

Table 13. XRD results for the reference concrete with RHA compared to concretes subjected to different temperature rises.

Mineral	Chemical formula	Acronym	RHA Ref	RHA 200°	RHA 300°	RHA 400°
Quartz	SiO_2	Q	46	56	66	55
Tobermorite	$Ca_5Si_6O_{16}(OH)_2.4H_2O$	T	32	35	18	18
Portlandite	$Ca(OH)_2$	P	1	1	0	0
Ettringite	$3CaO.Al_2O_3.3CaSO_4.32H_2O$	E	15	7	14	12
Gypsum	$CaSO_4.2H_2O$	G	6	2	2	15

According to Table 13, the hydrated calcium silicate (tobermorite) decomposed right after the temperature of 200 °C due to the loss of water from the structure, generating the release of silica oxide due to the dehydration of the CH [33]. The degradation of portlandite is observed in concretes shortly after exposure above 300 °C, as well as the degradation of gypsum after its exposure to temperatures greater than 200 °C.

Both the analyses for concrete molded with SF and for those composed of RHA show the decomposition of hydrated calcium silicate, which is the main compound responsible for the mechanical strength of concrete in general, in addition to the formation of other oxides that do not contribute to the gain on the load capacity of UHPC.

4. Conclusions

This work aimed to analyze the behavior of UHPC using two types of pozzolanic materials – SF and RHA.

For the mechanical performance, both had similar resistance capacities even after the analysis of age progression, being the difference in axial resistance between the materials being about 10 % greater for the concretes composed of RHA. This result for the sample group and due to the curing methodology applied to the specimens presents equal performance between the materials.

Analyzing permeability, this factor becomes important to determine the performance of products against the durability of UHPC. It was identified that even with the variation of the results between the concretes molded with SF and with RHA in the capillary permeability test, this factor depends on the structure of the pores of the materials, because the different concretes present water absorption levels and indices of analogous voids. As a repair material, the choice of a matrix composed of SF would be the most indicated since the propensity for fluid penetration due to permeability is lower than that of concrete made of RHA.

To analyze the behavior of the material in aggressive environments, after subjecting the concrete to sulfate attack, it was possible to observe a significant difference in the behavior when the samples were molded with SF and when they were made of RHA since the first pozzolan allowed a greater penetration of ions than compared to RHA, about 50 % higher. This may be due to the pore structure of this type of cementitious matrix, which, according to the results obtained by the XRD analysis, influenced the chemical composition of the material because of the more significant attack in concrete composed of SF. If thinking of an application as a repair material for structural recovery, concrete composed of RHA would be more indicated because of the lower propensity to suffer from this phenomenon in aggressive environments.

From the point of view of the mechanical behavior of concretes in situations where they undergo a significant temperature rise, for both analyzed compositions, the performance of concretes is presented the same. According to the analysis of variance adopted, the mechanical resistances of the different cementitious matrices are equivalent, and the microscopic evaluation using XRD demonstrates the chemical decomposition of the agents responsible for the mechanical resistance of the materials for both pozzolans.

Taking the analysis carried out in this work, the replacement of SF by RHA does not interfere with the mechanical performance of UHPC. Therefore, with the results obtained in this work, the application of any of the two pozzolans to produce concrete should be determined based on the aggressiveness class or the environment in which the material is expected to be used.

References

1. Sieg, A.P.A. et al. Concreto de pós-reativos – estudo das adições minerais: Cinza de casca de arroz, metacaulim e sílica ativa. Anais do 54° Congresso Brasileiro do Concreto. Maceió, 2012. Pp. 1–15.

2. Tayeh, B.A., Abu Bakar, B.H., Megat Johari, M.A., Voo, Y.L. Utilization of Ultra-high Performance Fibre Concrete (UHPFC) for Rehabilitation – A Review. Procedia Engineering. 2013. 54. Pp. 525–538. DOI: 10.1016/j.proeng.2013.03.048
3. Yoo, D., Yoon, Y. A Review on Structural Behavior, Design, and Application of Ultra-High-Performance Fiber-Reinforced Concrete. International Journal of Concrete Structures and Materials. 10(2). Pp. 125–142, 2016. DOI: 10.1007/s40069-016-0143-x
4. Yalçınkaya, Ç., Çopuroğlu, O. Hydration heat, strength and microstructure characteristics of UHPC containing blast furnace slag. Journal of Building Engineering. 2021. 34. Article no. 101915. DOI: 10.1016/j.jobe.2020.101915
5. Chen, Y., Yu, R., Wang, X., Chen, J., Shuiet, Zh. Evaluation and optimization of Ultra-High Performance Concrete (UHPC) subjected to harsh ocean environment: Towards an application of Layered Double Hydroxides (LDHs). Construction and Building Materials. 2018. 177. Pp. 51–62. DOI: 10.1016/j.conbuildmat.2018.03.210
6. Bajaber, M., Hakeem, I. UHPC evolution, development, and utilization in construction: a review. Journal of Materials Research and Technology. 2021. 10. Pp. 1058–1074. DOI: 10.1016/j.jmrt.2020.12.051
7. LI, J., Wu, Z., Shi, C., Yuan, Q., Zhang, Z. Durability of ultra-high performance concrete – A review. Construction and Building Materials. 2020. 255. Article no. 119296. DOI: 10.1016/j.conbuildmat.2020.119296
8. Mai, V.C., Luu, X.B., Nguyen, V.T. Ultra high-performance fiber reinforced concrete panel subjected to high velocity impact. Magazine of Civil Engineering. 2021. 107(7). Article no. 10703. DOI: 10.34910/MCE.107.3
9. Reddy, G.G.K., Ramadoss, P. Influence of alccofine incorporation on the mechanical behavior of ultra-high performance concrete (UHPC). Materials Today: Proceedings. 2020. 33(1). Pp. 789–79. DOI: 10.1016/j.matpr.2020.06.180
10. Abbas, S., Nehdi, M.L., Saleem, M.A. Ultra-High Performance Concrete: Mechanical Performance, Durability, Sustainability and Implementation Challenges. International Journal of Concrete Structures and Materials. 2016. 10. Pp. 271–295. DOI: 10.1007/s40069-016-0157-4
11. Wang, D., Shi, C., Wu, Z., Xiao, J., Huang, Zh., Fang, Zh. A review on ultra-high-performance concrete: Part II. Hydration, microstructure and properties. Construction and Building Materials. 2015. 96. Pp. 368–377. DOI: 10.1016/j.conbuildmat.2015.08.095
12. Lessly, S.H., Lakshmana Kumar, S., Raj Jawahar, R., Prabhu, L. Durability properties of modified ultra-high performance concrete with varying cement content and curing regime. Materials Today: Proceedings. 2021. 45(7). Pp. 6426–6432. DOI: 10.1016/j.matpr.2020.11.271
13. Abid, M., Hou, X., Zheng, W., Hussain, R.R. High temperature and residual properties of reactive powder concrete – A review. Construction and Building Materials. 2017. 147. Pp. 339–351. DOI: 10.1016/j.conbuildmat.2017.04.083
14. Rawat, S., Lee, C.K., Zhang, Y.X. Performance of fiber-reinforced cementitious composites at elevated temperatures: A review. Construction and Building Materials. 2021. 292. Article no. 123382. DOI: 10.1016/j.conbuildmat.2021.123382
15. Romano, R.C.O., Schreurs, H., John, V.M., Pileggi, R.G. Influência da técnica de dispersão nas propriedades de silica ativa. Cerâmica. 2008. 54(332). Pp. 456–461. DOI: 10.1590/S0366-69132008000400011
16. Fraga, Y.S.B., Rêgo, J., Capuzzo, V.M.S., da Silva Andrade, D. Efeito da ultrasonicação da sílica ativa e da nanossílica colloidal em pastas de cimento. Matéria (Rio de Janeiro). 2020. 25(4). DOI: 10.1590/s1517-707620200004.1147
17. ABNT. NBR 5739: Concreto – ensaio se compressão de corpos-de-prova cilíndricos. Associação brasileira de normas técnicas. Rio de Janeiro, 2007. 4 p.
18. ABNT. NBR 9778: Argamassa e concreto endurecidos – determinação da absorção de água, índices de vazios e massa específica. Associação brasileira de normas técnicas. Rio de Janeiro, 2005. 4 p.
19. ABNT. NBR 9779: Argamassa e concreto endurecidos – determinação da absorção de água por capilaridades. Associação brasileira de normas técnicas. Rio de Janeiro, 2012. 3 p.
20. Mazer, W., Macioski, G.; Soto, N. Determinação de ions sulfato em estruturas de concreto. Blucher Chemical Engineering Proceedings. 2015. 1(2). Pp. 13574–13580.
21. ABNT. NBR 16937-6: Águas agressivas – durabilidade do concreto. parte 6: Determinação de sulfato solúvel em água. Associação brasileira de normas técnicas. Rio de Janeiro, 2021. 6 p.
22. ABNT. NBR 14432: Exigências de Resistencia ao fogo de elementos construtivos de edificações – procedimento. Associação brasileira de normas técnicas. Rio de Janeiro, 2001. 14 p.
23. Ganasini, D. Concretos de Alto Desempenho reforçado com microfibras de polipropileno e submetidos a elevadas temperaturas. 135 p. Dissertação (Mestrado) — Centro de Ciências Tecnológicas, Programa de Pós-Graduação em Engenharia Civil. Universidade do Estado de Santa Catarina., Joinville, 2019.
24. Lee, N. et al. Microstructural investigation of calcium aluminate cement-based ultra-high performance concrete (uhpc) exposed to high temperatures. Cement and Concrete Research. v. 102. p. 109–118. 2017. ISSN 0008-8846.
25. Ju, Y. et al. Experimental investigation of the effect of silica fume on the thermal spalling of reactive powder concrete. Construction and Building Materials. v. 155. Pp. 571–583. 2017. ISSN 0950-0618.
26. Zhang, D., Tan, K.H. Effect of various polymer fibers on spalling mitigation of ultra-high performance concrete at high temperature. Cement and Concrete Composites. v. 114. Pp. 103815. 2020. ISSN 0958-9465.
27. Bulgakov, B.I., Nguyen, V.Q.D., Aleksandrova, A.V., Larsen, O.A., Galtseva, N.A. High-performance concrete produced with locally available materials. Magazine of Civil Engineering. 2023. 117(1). Article No. 11702. DOI: 10.34910/MCE.117.2
28. Lesovik, V.S., Popov, D.Y., Fediuk, R.S., Sabri, M.M., Vavrenyuk, S.V., Liseitsev, Y.L. Shrinkage of ultra-high performance concrete with superabsorbent polymers. Magazine of Civil Engineering. 2023. 121(5). Article No. 12108. DOI: 10.34910/MCE.121.8
29. Dinakar, P., Sahoo, P.K., Sriram, G. Effect of metakaolin content on the properties of high strength concrete. International Journal of Concrete Structures and Materials. v. 7. p. 215–223. 2013. ISSN 1976-0485.
30. De Medeiros-Junior, R.A., Munhoz, G. da S., de Medeiros, M.H.F. Correlations between water absorption, electrical resistivity and compressive strength of concrete with different contents of pozzolan. Revista ALCONPAT. 2019. 9(2). Pp. 152–166. https://doi.org/10.21041/ra.v9i2.335.
31. Sun, D., Wu, K., Shi, H., Zhang, L., Zhang, L. Effect of interfacial transition zone on the transport of sulfate ions in concrete. Construction and Building Materials. 2018. 192. Pp. 28–37. DOI: 10.1016/j.conbuildmat.2018.10.140

32. Zheng, W., Luo, B., Wang, Y. Compressive and tensile properties of reactive powder concrete with steel fibers at elevated temperatures. Construction and Building Materials. 2013. 41. Pp. 844–851. DOI: 10.1016/j.conbuildmat.2012.12.066
33. Zou, D., Qin, Sh., Liu, T., Jivkov, A. Experimental and Numerical Study of the Effects of Solution Concentration and Temperature on Concrete under External Sulfate Attack. Cement and Concrete Research. 2021. 139. Article no. 106284. DOI: 10.1016/j.cemconres.2020.106284

Information about the authors:

Elizamary Otto Ferreira,
ORCID: https://orcid.org/0000-0002-2262-7424
E-mail: elizamaryotto@gmail.com

Alessandra Tourinho Maia,
ORCID: https://orcid.org/0000-0003-2168-4301
E-mail: alessandra.tourinho@gmail.com

Wellington Mazer, *Doctor of Science*
ORCID: https://orcid.org/0000-0002-9941-999X
E-mail: wmazer@utfpr.edu.br

Received 15.12.2023. Approved after reviewing 19.11.2025. Accepted 20.11.2025.